



1 **Comparison of Vaisala radiosondes RS41 and RS92 in**  
2 **the oceans ranging from the Arctic to tropics**

3  
4 **Yoshimi Kawai<sup>1</sup>, Masaki Katsumata<sup>1</sup>, Kazuhiro Oshima<sup>2</sup>, Masatake E. Hori<sup>2</sup>, and Jun**  
5 **Inoue<sup>3</sup>**

6  
7 <sup>1</sup>Research and Development Center for Global Change, Japan Agency for Marine–Earth  
8 Science and Technology, Yokosuka 237-0061, Japan

9 <sup>2</sup>Institute of Arctic Climate and Environment Research, Japan Agency for Marine–Earth  
10 Science and Technology, Yokosuka 237-0061, Japan

11 <sup>3</sup>Arctic Environment Research Center, National Institute of Polar Research, Tachikawa  
12 190-8518, Japan

13  
14

15 *Correspondence to:* Yoshimi Kawai (ykawai@jamstec.go.jp)

16

17 **Abstract.** To assess the differences between the RS92 radiosonde and its improved  
18 counterpart, the Vaisala RS41-SGP radiosonde that has a pressure sensor, 36  
19 twin-radiosonde launches were made over the Arctic Ocean, Bering Sea, northwestern  
20 Pacific Ocean, and the tropical Indian Ocean during two cruises of the R/V *Mirai* in 2015.  
21 The biases, standard deviations, and root mean squares (RMSs) of the differences



22 between the RS41 and RS92 data over all flights and altitudes were smaller than the  
23 nominal combined uncertainties of the RS41, except that the RMS of the differences of  
24 pressure above 100 hPa exceeded 0.6 hPa. A comparison between daytime and nighttime  
25 flights in the tropics revealed that the pressure difference was systematically larger during  
26 the day than at night above an altitude of 4.5 km, the suggestion being that there was some  
27 effect of solar heating on the pressure measurements, but the exact reason is unclear. The  
28 agreement between the RS41 and RS92 temperature measurements was better than the  
29 combined uncertainties. However, there were some noteworthy discrepancies that were  
30 presumably caused by the “wet-bulbing” effect and stagnation of the balloon. Although the  
31 median of the relative humidity differences was only a little more than 2 % of the relative  
32 humidity at all altitudes, the relative humidity of the RS92 was much lower than that of the  
33 RS41 at altitudes of about 17 km in the tropics. This dry bias might have been caused by  
34 the incomplete solar radiation correction of the RS92, and a correction table for the daytime  
35 RS92 humidity was calculated. This study showed that the RS41 measurements were  
36 consistent with the specifications of the manufacturer in most cases over both the tropical  
37 and polar oceans. However, further studies of the causes of the discrepancies are needed.

38



## 39 **1 Introduction**

40 Radiosonde observations are regularly conducted twice a day at about 800 sites  
41 throughout the world. Radiosondes measure temperature, humidity, wind velocities, and  
42 pressure (or height) in the troposphere and stratosphere. They ascend through the  
43 atmosphere attached to balloons filled with helium. The data are sent to the global  
44 telecommunication system and are used for data assimilation in real-time operational  
45 weather forecast systems, atmospheric reanalyses, and climate models. In situ aerological  
46 observations are also indispensable for validating satellite-derived meteorological data (e.g.  
47 Fujita et al., 2008), for assessing long-term trends in the upper atmosphere (e.g. Thorne et  
48 al., 2005; Maturilli and Kayser, 2016), and for other meteorological research, including  
49 assimilation experiments and air-sea interaction studies (e.g. Inoue et al., 2013; 2015;  
50 Kawai et al., 2014). Efforts to enhance the reliability of radiosonde data have continued to  
51 the present time (e.g. Ciesielski et al., 2014; Bodeker et al., 2016). One consequence of the  
52 technological advancements has been the need to account for accuracy differences  
53 following radiosonde upgrades in the long-term continuous datasets.

54 The model RS92 radiosonde manufactured by Vaisala Ltd., which was first introduced  
55 in 2003, has been used throughout the world, and it is now being replaced with a successor  
56 model, the RS41 (Table 1). To clarify the differences between the RS41 and RS92  
57 radiosondes, intercomparison experiments have already been carried out at several sites  
58 on land from high latitudes to the tropics (Mötl, 2014; Jauhiainen et al., 2014; Jensen et al.,



59 2016). Jauhiainen et al. (2014) have reported results of comparisons in several countries,  
60 including Finland, the United Kingdom, the Czech Republic, and Malaysia. They reported  
61 that the RS41 radiosonde was a consistent improvement over the RS92 in terms of  
62 reproducibility with respect to temperature and humidity under both day and night  
63 conditions. A different intercomparison study was carried out at a site in Oklahoma, USA, by  
64 Jensen et al. (2016). They showed that the RS92 and RS41 measurements agreed much  
65 better than the manufacturer-specified combined uncertainties. Their results also indicated  
66 that the RS41 measurements of temperature and humidity appeared to be less sensitive to  
67 solar heating than those made with the RS92.

68 The accuracy of the pressure measured with the model RS41-SGP, however, has not  
69 yet been examined, nor has a comparison been made between the RS41 and RS92  
70 radiosondes in the marine atmosphere. Unlike the atmosphere over land, the marine  
71 atmosphere is less affected by topography and the greater temperature variations of the  
72 land surface. As a result, phenomena such as convection and precipitation and their diurnal  
73 cycles over the oceans are different from those over land (e.g. Yang and Slingo, 2001;  
74 Minobe and Takebayashi, 2015). We performed a total of 36 intercomparison flights during  
75 two cruises of R/V *Mirai* of the Japan Agency for Marine-Earth Science and Technology  
76 (JAMSTEC) in 2015. Our observations covered a wide range of latitudes over the oceans,  
77 an important consideration from the standpoint of confirming the performance of the RS41.  
78 We describe the cruises and the methodology of the intercomparison observations in Sect.



79 2. Section 3 shows the results of the comparisons. In Sect. 4, we focus on the data obtained  
80 in the tropics and further discuss the reasons for the differences between the RS41 and  
81 RS92 results. Section 5 is a summary of the study.

## 82 **2 Intercomparison experiment**

### 83 **2.1 Cruises**

84 The intercomparison observations were performed by launching both the RS41 and RS92  
85 radiosondes tied to one balloon (referred to as a “twin-radiosonde” flight) during the  
86 MR15-03 and MR15-04 cruises of R/V *Mirai*. In the case of the MR15-03 cruise, the vessel  
87 departed from Hachinohe, Japan, on 26 August, cruised the Arctic Ocean from 6  
88 September to 3 October (Nishino et al., 2015), and returned to Hachinohe on 21 October.  
89 The twin-radiosonde flights were launched 9 times in the Chukchi Sea, 4 times in the Bering  
90 Sea, and 5 times in the northwestern Pacific (Fig. 1a and Table 2). The MR15-04 cruise  
91 was for tropical meteorological research, and the vessel stayed near 4°04' S, 101°54' E off  
92 Bengkulu, west of Sumatra Island, in the Indian Ocean during 23 November to 17  
93 December for stationary observations, including 16 twin-radiosonde flights (Katsumata et  
94 al., 2015). We also conducted intercomparison observations twice in the western Pacific on  
95 the way from Japan to the site off Sumatra (Fig. 1b and Table 2).

### 96 **2.2 Methods**



97 We used radiosonde models RS92-SGPD and RS41-SGP in this study. Their nominal  
98 accuracies are summarized in Table 1. Whereas the RS41-SG radiosonde used in the  
99 previous studies (Motl, 2014; Jauhainen et al., 2014; Jensen et al., 2016) derived pressure  
100 from Global Positioning System (GPS) data with no pressure sensor, the RS41-SGP has a  
101 pressure sensor consisting of a silicon capacitor. The pressure and height data analyzed in  
102 this study were measured directly and derived from the hypsometric equation, respectively.  
103 Note that GPS-derived pressure and height were not used, unlike in the previous studies.  
104 Two different DigiCORA systems were used on R/V *Mirai* for the simultaneous RS92 and  
105 RS41 soundings. The receiving system (MW41) used for the RS41 included a processor  
106 (SPS331), processing and recording software (MW41 v2.2.1), GPS antenna (GA20), and  
107 UHF antenna (RB21), which was part of the ASAP sounding station permanently installed  
108 on R/V *Mirai*. The RS41 sensors were calibrated with a new calibrator (RI41) and a  
109 barometer (PTB330). In contrast, we used a previous generation system for the RS92: the  
110 receiving system (MW31) included a processor (SPS311), software (DigiCORA v3.64),  
111 GPS antenna (GA31), and UHF antenna (RM32). The instrumentation was temporarily  
112 placed in or on the aft wheelhouse. The RS92 sensors were calibrated with a calibrator  
113 (GC25) and a PTB330 barometer. Because version 3.61 of DigiCORA was incorrectly used  
114 during the cruises, all RS92 sounding data were simulated with DigiCORA v3.64 after the  
115 cruises.

116 The RS41 and RS92 radiosondes were directly attached to each other with sticky



117 tape (Fig. 2) instead of hanging them from the two ends of a rod (Jensen et al., 2016) to  
118 facilitate the launching operations on the rocking ship deck. The two radiosondes were  
119 hung from a single 350g Totex balloon with the cord of the RS41 radiosonde. The ascent  
120 rates were approximately  $5 \text{ m s}^{-1}$  and  $4 \text{ m s}^{-1}$  during the MR15-03 and MR15-04 cruises,  
121 respectively (Table 2). Whereas nighttime twin-radiosonde flights could be carried out only  
122 once during the MR15-03 cruise owing to operations associated with oceanographic  
123 observations, we performed eight nighttime flights during the MR15-04 cruise (Fig. 1c and  
124 Table 2).

125 During flight No. 33 (02:50 UTC on 16 Dec.), the radiosondes moved up and down  
126 around a temperature of  $0^\circ\text{C}$ , perhaps because the balloon froze, and only the data before  
127 the up-and-down motion were analyzed in this study. In the case of flight No. 9 (05:30 UTC  
128 on 16 Sep.), we delayed the measurement time of the RS41 by 17 s in the analysis  
129 because the twin radiosondes flew horizontally just after launching, and the automatic  
130 determinations of the starting times disagreed between the RS92 and RS41. Because the  
131 pressure values measured with the PTB330 barometer for the calibration of the RS92 had a  
132 bias of 0.18 hPa before the launch of the No. 5 radiosondes, we subtracted 0.18 hPa from  
133 the observed pressure values of the RS92 No. 1–4 radiosondes when the data were  
134 analyzed. The balloon release detection mode was changed from automatic to manual  
135 during the MR15-04 cruise, and the starting times of the RS92 and RS41 radiosondes  
136 during the MR15-04 cruise generally appeared to differ slightly. Therefore, the



137 measurement times of all the RS92 radiosonde data during the MR15-04 cruise were  
138 delayed by 1.7 s in the analysis.

### 139 **3 Results**

140 For easier comparison with the results of Jensen et al. (2016), we interpolated the RS92  
141 radiosonde profiles to the same time step as the RS41 profiles, and calculated differences  
142 between them at each 10-m vertical grid based on the RS41 radiosonde heights (Fig. 3).  
143 The vertical axis of Fig. 3 is therefore nearly equivalent to the passage of time. The biases,  
144 standard deviations, and root mean square (RMS) differences were all smaller than the  
145 combined uncertainties, except that the RMS differences of pressure above 100 hPa  
146 exceeded 0.6 hPa (Table 3). For temperature and wind speeds, the biases and RMS  
147 differences in our experiments were nearly the same as those of Jensen et al. (2016), but  
148 the differences of pressure and relative humidity were much larger in our study.

#### 149 **3.1 Pressure**

150 The pressure difference between the RS41 and RS92 radiosondes increased as the  
151 radiosondes rose to an altitude of about 5 km but averaged an almost constant 0.5–0.6 hPa  
152 above that altitude (Fig. 3a). The 90th-percentile line revealed that the sensor-measured  
153 RS41 pressure was lower than the RS92 for more than 90 % of the measurements above 5  
154 km. The percentage of the pressure differences that exceeded the combined uncertainty  
155 (Table 1) was 13.7 % below 100 hPa but 50.9 % above 100 hPa.



156 **3.2 Relative humidity**

157           The median of the relative humidity differences peaked at approximately 2 %RH near  
158 10 km (Fig. 3b), a result consistent with the data of Jensen et al. (2016). The humidity  
159 difference was also large near the sea surface in our analysis. For 13.0 % of the  
160 measurements, the absolute value of the difference exceeded 4.0 %RH, which is the  
161 combined uncertainty of the RS41-SGP. One noteworthy feature of Fig. 3b is that there  
162 were quite large differences of relative humidity at a height of about 17 km, although the  
163 median difference was less than 0.5 %RH. Figure 4 shows the relationship between the  
164 humidity difference and temperature for each category of relative humidity. During both the  
165 MR15-03 and MR15-04 cruises, the RS41 radiosonde tended to record a higher mean  
166 relative humidity than the RS92 for all humidity ranges. The humidity difference peaked at  
167 around  $-40^{\circ}\text{C}$ , a pattern similar to Fig. 17 of Jensen et al. (2016). The differences were  
168 relatively small in the range of  $-50^{\circ}$  to  $-70^{\circ}\text{C}$ , but the RS41 humidity was much higher than  
169 the RS92 at temperatures below  $-80^{\circ}\text{C}$  (Fig. 4b). The atmosphere associated with  
170 temperatures below  $-80^{\circ}\text{C}$  corresponds to the tropopause in the tropics, where the greatest  
171 differences were apparent at altitudes of about 17 km (Fig. 3b).

172 **3.3 Temperature**

173 In the case of temperature, although there was a slight positive bias below an altitude of 10  
174 km, the median of the differences was within  $\pm 0.12^{\circ}\text{C}$  below an altitude of 26 km (Fig. 3c).



175 The median exceeded  $0.5^{\circ}\text{C}$  above 27 km, but only four flights reached that height, and the  
176 large median was attributable to differences on two of the flights (No. 23 and 24). The  
177 percentages of the temperature difference that exceeded the combined uncertainty were  
178 4.0 % below 16 km and 5.9 % above 16 km. Figure 3c also shows that the standard  
179 deviation of the temperature differences was smaller at altitudes below 16 km, but there  
180 were quite large standard deviations near the surface and at altitudes of about 1.3 km and  
181 5.3 km because of some outliers. The extreme temperature difference, which reached  
182  $2.75^{\circ}\text{C}$  at an altitude of 1.27 km, was observed on 10 December in the tropics (Fig. 5a).  
183 The RS92 temperature became much lower than the RS41 just after the radiosondes  
184 passed through a saturated layer into a dry layer. The greater reduction of the RS92  
185 temperature was probably due to the “wet-bulbing” effect mentioned by Jensen et al. (2016),  
186 who indicated that the sequential pulse heating method with relatively long non-heating  
187 periods may not be sufficient to eliminate icing/wetting of the RS92 sensor. A large  
188 temperature difference that was likely caused by the wet-bulbing effect was also observed  
189 in a sounding in the Arctic, although the maximum difference was less than  $0.75^{\circ}\text{C}$  (Fig.  
190 5b).

191 Figure 6 shows the cases of extreme temperature differences that contributed to the  
192 greater standard deviation and cannot be explained by the wet-bulbing effect. For the flight  
193 on 11 December (Fig. 6a), there was a large temperature discrepancy inside the saturated  
194 layer. In that case, the radiosondes were launched in heavy rain, and the ascent rate



195 dropped to nearly zero at approximately 5.4 km, probably because of rain or snow and  
196 freezing of the balloon. Furthermore, the horizontal wind speed was less than  $3.0 \text{ m s}^{-1}$   
197 around this altitude. As a result, the temperature sensors were presumably not ventilated  
198 sufficiently. In the case of the flights on 1 and 3 December (Fig. 6b and 6c), the RS41  
199 temperatures were higher than the RS92 by more than  $1.0^\circ\text{C}$  near the surface. Because  
200 the surface reference air temperatures were close to the RS92 temperatures at the lowest  
201 level, we suspect that the RS41 temperatures were too high. Yoneyama et al. (2002) have  
202 indicated that ship body heating can affect radiosonde sensors. However, that effect was  
203 restricted to within several tens of meters of the sea surface in their experiments. Although  
204 we cannot completely exclude the possibility that the temperature sensors of the two RS41  
205 radiosondes were improperly heated by the body of the ship or direct insolation or improper  
206 handling near the surface, the reason for these large discrepancies remains unclear.

### 207 **3.4 Wind speed**

208 Vertical profiles of the wind speed differences are shown in Fig. 3d and 3e. The  
209 percentages of the differences in the zonal and meridional wind speeds that exceeded  $0.5$   
210  $\text{m s}^{-1}$  were 1.9 % and 1.5 %, respectively. Although both the zonal and meridional wind  
211 speeds agreed to within  $0.5 \text{ m s}^{-1}$  for almost all measurements, several spikes can be seen  
212 in the standard deviations and percentiles. In half of all flights, the magnitude of the  
213 difference of the horizontal wind speed exceeded  $1.0 \text{ m s}^{-1}$  for a brief moment. The wind



214 speed data in our soundings were noisier than those reported by Jensen et al. (2016).

215

## 216 **4 Discussion**

### 217 **4.1 Day-night differences**

218 Figure 7 compares the differences between daytime (10 flights) and nighttime (8 flights) for  
219 the soundings during the MR15-04 cruise. The median of the pressure difference was  
220 greater in the day than at night above an altitude of 4.5 km (Fig. 7a). The median of the  
221 nighttime differences was close to that of the daytime flights in the Arctic cruise below an  
222 altitude of 15 km, the implication being that the day-night difference might reflect some  
223 effect of solar heating.

224 The median profiles of temperature differences in the day and night were close to  
225 each other, with slightly larger differences in the night at altitudes of 5–15 km (Fig. 7b). The  
226 daytime difference became greater above approximately 24 km, a pattern similar to the  
227 results of Jensen et al. (2016). According to them, the difference in the radiation correction  
228 schemes between the RS92 and RS41 may be the dominant cause of these temperature  
229 differences, particularly at high solar elevation angles and low pressures.

230 The median of the relative humidity difference was larger during the day than at night  
231 from the surface to an altitude of 20 km and was especially large at an altitude of about 17  
232 km (Fig. 7c). The very large difference (RS41 > RS92) in relative humidity around the



233 tropopause shown in Figs. 3c and 4b occurred in the daytime. This pattern is consistent  
234 with the results of Jauhiainen et al. (2014), who indicated that the difference was largely  
235 due to the dissimilar approaches used to compensate for the heating effect of solar  
236 radiation on the humidity sensor. Similar dry biases were reported for the RS92 radiosonde  
237 with the earlier version of DigiCORa (Vömel et al., 2007; Yoneyama et al., 2008), although  
238 the dry bias was absent from later observations (Ciesielski et al., 2014; Yu et al., 2015).  
239 Figure 8 shows the relative difference of relative humidity in the daytime between the RS92  
240 and RS41 radiosondes. The relative difference is defined to be the relative humidity  
241 difference expressed as a percentage of the RS41 relative humidity. The relative difference  
242 was small in the lower troposphere and became greater as the radiosondes rose higher. Its  
243 median peaked at  $-36.9\%$  at an approximate altitude of 19 km. This pattern of the vertical  
244 profile of relative difference is similar to that between the RS92 radiosonde and a reference  
245 instrument shown by Vömel et al. (2007), but the values in Fig. 8 are less than half of those  
246 in Fig. 6 of Vömel et al. (2007).

#### 247 **4.2 Humidity correction**

248 Figures 7c and 8 imply that a small dry bias still remains in the RS92 radiosonde  
249 observations. We attempted to correct the RS92 relative humidity obtained during the  
250 MR15-04 cruise by using the RS41 as a reference instrument. We used the cumulative  
251 distribution function (CDF) matching method proposed by Ciesielski et al. (2009) to make



252 the correction. The details of this method can be found in Ciesielski et al. (2009). We first  
253 created CDFs of relative humidity for the RS92 and RS41 using temperature bins of 20°C  
254 between +30° and -90°C (10 to 30°C, -10 to 10°C, -30 to -10°C, -50 to -30°C, -70 to  
255 -50°C, and -90 to -70°C) using 5hPa radiosonde data in 5%RH intervals. Figure 9 shows  
256 the CDFs of the RS92 and RS41 in the temperature range -90 to -70°C as an example.  
257 The frequency of lower relative humidity was greater for the RS92 in this temperature range,  
258 which includes the tropopause (Fig. 9a). We then, for example, paired the RS92 value of  
259 27.50 %RH at the 71.23th percentile with the corresponding RS41 value at this same  
260 percentile. The RS41 relative humidity at the 71.23th percentile was 36.43 %RH, and the  
261 difference between 36.43 %RH and 27.50 %RH (= +8.93 %RH) was the bias correction for  
262 the RS92 value of 27.5 %RH. Figure 9b shows the bias correction over the entire relative  
263 humidity range for temperatures of -90 to -70°C.

264 Table 4 shows the daytime bias correction for the entire ranges of temperature and  
265 relative humidity. The correction was seldom more than 5 %RH when the RS92  
266 temperature exceeded -60°C. The correction was large for RS92 radiosonde values in the  
267 range 15–50 %RH and temperatures of -80°C, with a maximum of +8.93 %RH. This  
268 pattern is similar to that of the correction table for the RS80 radiosonde in the daytime  
269 reported by Ciesielski et al. (2010) (their Fig. 7b), but the values in Table 4 are much smaller.  
270 We corrected the daytime RS92 relative humidity values obtained during the MR15-04  
271 cruise using Table 4. The correction value for an arbitrary RS92 measurement can be



272 obtained by linear two-dimensional interpolation using Table 4 and the RS92 temperature  
273 and relative humidity. Figure 10 shows median profiles of the differences between the RS92  
274 and RS41 radiosondes before and after the correction. Although the median of the  
275 magnitude of the differences still exceeded 2.0 %RH around 120, 150, and 560 hPa, most  
276 of the medians were within  $\pm 1.0$  %RH. The mean of the relative humidity difference of the  
277 5hPa interval data was  $-2.02$  %RH if no correction was made; this difference was reduced  
278 to  $-0.01$  %RH after the correction.

## 279 **5 Conclusions**

280 To examine differences between the RS41 and RS92 radiosondes, a total of 36  
281 twin-radiosonde flights were performed over the Arctic Ocean, Bering Sea, northwestern  
282 Pacific Ocean, and the tropical Indian Ocean during two cruises of R/V *Mirai* in 2015. We  
283 used the model RS41-SGP radiosonde, which has a pressure sensor, unlike previous  
284 studies that used the RS41-SG, which has no pressure sensor.

285 The biases, standard deviations, and RMS of the differences between the RS41 and  
286 RS92 over all flights and heights were smaller than the nominal combined uncertainties of  
287 the RS41, except that the RMS differences of pressure above 100 hPa exceeded 0.6 hPa.  
288 Whereas the biases and the RMS differences of temperature and wind speeds were close  
289 to those reported by Jensen et al. (2016), the differences of pressure and relative humidity  
290 were greater in our experiments. The pressure difference increased as the radiosondes



291 rose higher; the median and mean were 0.5–0.6 hPa at altitudes above 5 km. A comparison  
292 between daytime and nighttime flights in the tropics revealed that the pressure difference  
293 was systematically larger in the day than at night at altitudes above 4.5 km, the suggestion  
294 being that there was some effect of solar heating on the pressure measurements. The  
295 exact reason, however, is unclear.

296 The RS41 and RS92 temperature measurements in general agreed better than the  
297 combined uncertainties, but there were some noteworthy exceptions. One possible reason  
298 for the noteworthy discrepancies is the wet-bulbing effect described by Jensen et al. (2016).  
299 In a dry layer just above a saturated layer, the RS92 temperature sensor was cooled too  
300 much by evaporation. The RS41 temperature appeared to be less sensitive to this  
301 wet-bulbing effect. This phenomenon was confirmed in both the tropics and Arctic. During  
302 heavy rain and weak wind conditions, the stagnation of the balloon probably suppressed  
303 the ventilation around the temperature sensors, the result being an extreme temperature  
304 difference.

305 The median of the relative humidity differences at all altitudes was only a little more  
306 than 2 %RH. However, there were quite large differences at an altitude of about 17 km.  
307 These large differences occurred in the daytime around the tropical tropopause, where the  
308 temperature was below  $-80^{\circ}\text{C}$ . The reason for this dry bias may be that there was some  
309 remnant of the error of the RS92 radiosonde solar radiation correction. We attempted to  
310 correct the RS92 relative humidity data obtained in the daytime during the MR15-04 cruise



311 by using the CDF matching method, and the corrected RS92 relative humidity agreed well  
312 with the RS41 values.

313 Our results showed that measurements with the RS41 radiosonde satisfied the  
314 performance specifications of the manufacturer in most cases over both the tropical and  
315 polar oceans. The RS41 temperature and humidity sensors appeared to be unaffected by  
316 the solar radiation correction error and the wet-bulbing effect. Some concerns, however,  
317 remain. Specifically, the reasons for the pressure bias in the upper layer and the two cases  
318 of extreme temperature discrepancies that occurred below an altitude of several hundred  
319 meters are unknown. Further experiments will be necessary to address these issues, and  
320 users should be cognizant of these concerns.

## 321 **6 Data availability**

322 The sounding dataset and the ship-observed surface meteorology are expected to be  
323 released just two years after the cruises (October 2017 for the MR15-03, and December  
324 2017 for the MR15-04) from the website of the Data Research System for Whole Cruise  
325 Information (DARWIN) in JAMSTEC (<http://www.godac.jamstec.go.jp/darwin/e>) in accord  
326 with the cruise data policy of JAMSTEC.

327

## 328 **Author contributions**

329 All co-authors contributed to designing the experiments and preparing for the observation



330 cruises. Y. Kawai, M. Katsumata, and K. Oshima participated in the R/V *Mirai* cruises and  
331 carried out the radiosonde soundings. K. Oshima reprocessed the RS92 data. Y. Kawai  
332 mainly analyzed the data and prepared the manuscript with contributions from all  
333 co-authors.

334

335 *Acknowledgments.* The authors sincerely thank the captains, crews, and observation  
336 technicians of the R/V *Mirai* and all colleagues who helped with the experiments. The  
337 authors are also grateful to K. Yoneyama of JAMSTEC for valuable advice, especially for  
338 advice concerning the humidity correction. This study was supported by the Japan Society  
339 for the Promotion of Science (JSPS) Grants-in-Aid for Scientific Research (A), (B), and (C)  
340 (KAKENHI) Grant Number 24241009, 16H04046, and 16K05563.

341

## 342 **References**

343 Bodeker, G. E., Bojinski, S., Cimini, C., Dirksen, R. J., Haeffelin, M., Hannigan, J. W., Hurst,  
344 D. F., Leblanc, T., Madonna, F., Maturilli, M., Mikalsen, A. C., Philpona, R., Reale, T.,  
345 Siedel, D. J., Tan, D. G. H., Thorne, P. W., Vömel, H., and Wang, J.: Reference upper-air  
346 observations for climate: From concept to reality, B. Am. Meteorol. Soc., 97, 123-135,  
347 doi:10.1175/BAMS-D-14-00072.1, 2016.

348 Ciesielski, P. E., Johnson, R. H., and Wang, J: Correction of humidity biases in Vaisala  
349 RS80-H sondes during NAME, J. Atmos. Ocean. Tech., 26, 1763-1780,



- 350 doi:10.1175/2009JTECHA1222.1, 2009.
- 351 Ciesielski, P. E., Chang, W.-M., Huang, S. -C., Johnson, R. H., Jou, B. J. -D., Lee, W. -C.,  
352 Lin, P. -H., Liu, C. -H., and Wang, J.: Quality-controlled upper-air sounding dataset for  
353 TIMREX/SoWMEX: Development and corrections, *J. Atmos. Ocean. Tech.*, 27,  
354 1802-1821, doi:10.1175/2010JTECHA1481.1, 2010.
- 355 Ciesielski, P. E., Yu, H., Johnson, R. H., Yoneyama, K., Katsumata, M., Long, C. N., Wang,  
356 J., Loehrer, S. M., Young, K., Williams, S. F., Brown, W., Braun, J., and Van Hove, T.:  
357 Quality-controlled upper-air sounding dataset for DYNAMO/CINDY/AMIE: Development  
358 and corrections, *J. Atmos. Ocean. Tech.*, 31, 741-764, doi:10.1175/JTECH-D-13-00165.1,  
359 2014.
- 360 Fujita, M., Kimura, F., Yoneyama, K., and Yoshizaki, M.: Verification of precipitable water  
361 vapor estimated from shipborne GPS measurements, *Geophys. Res. Lett.*, 35, L13803,  
362 doi:10.1029/2008GL033764, 2008
- 363 Inoue, J., Enomoto, T., and Hori, M. E.: The impact of radiosonde data over the ice-free  
364 Arctic Ocean on the atmospheric circulation in the Northern Hemisphere, *Geophys. Res.*  
365 *Lett.*, 40, 864-869, doi:10.1002/grl.50207, 2013.
- 366 Inoue, J., Yamazaki, A., Ono, J., Dethloff, K., Maturilli, M., Neuber, R., Edwards, P., and  
367 Yamaguchi, H.: Additional Arctic observations improve weather and sea-ice forecasts for  
368 the Northern Sea Route, *Sci. Rep.*, 5, 16868, doi:10.1038/srep16868, 2015.
- 369 Jauhiainen, H., Survo, P., Lehtinen, R., and Lentonen, J.: Radiosonde RS41 and RS92 key



370 differences and comparison test results in different locations and climates. TECO-2014,  
371 WMO Technical Conference on Meteorological and Environmental Instruments and  
372 Methods of Observations, Saint Petersburg, Russian Federation, 7–9 July 2014, P3(16),  
373 2014.

374 Jensen, P. M., Holdridge, D. J., Survo, P., Lehtinen, R., Baxter, S., Toto, T., and Johnson, K.  
375 L.: Comparison of Vaisala radiosondes RS41 and RS92 at the ARM Southern Great  
376 Plains site, Atmos. Meas. Tech., 9, 3115-3129, doi:10.5194/amt-9-3115-2016, 2016.

377 Katsumata, M., and coauthors: R/V Mirai Cruise Report MR15-04, Cruise Rep., Japan  
378 Agency for Marine-Earth Science and Technology, Yokosuka, Japan, 241.pp, 2015.  
379 (Available from  
380 [http://www.godac.jamstec.go.jp/catalog/data/doc\\_catalog/media/MR15-04\\_all.pdf](http://www.godac.jamstec.go.jp/catalog/data/doc_catalog/media/MR15-04_all.pdf))

381 Kawai, Y., Tomita, H., Cronin, M. F., and Bond, N. A.: Atmospheric pressure response to  
382 mesoscale sea surface temperature variations in the Kuroshio Extension: In situ  
383 evidence, J. Geophys. Res. Atmos., 119, 8015-8031. doi:10.1002/2013JD021126, 2014.

384 Maturilli, M., and Kayser, M.: Arctic warming, moisture increase and circulation changes  
385 observed in the Ny-Ålesund homogenized radiosonde record, Theor. Appl. Climatol.,  
386 doi:10.1007/s00704-016-1864-0, 2016.

387 Minobe, S., and Takebayashi, S.: Diurnal precipitation and high cloud frequency variability  
388 over the Gulf Stream and over the Kuroshio, Clim. Dyn., 44, 2079-2095,  
389 doi:10.1007/s00382-014-2245-y, 2015.



- 390 Motl, M.: Vaisala RS41 trial in the Czech Republic, Vaisala News, 192, 14-17, 2014.
- 391 Nishino, S., and coauthors: R/V Mirai Cruise Report MR15-03, Cruise Rep., Japan Agency  
392 for Marine-Earth Science and Technology, Yokosuka, Japan, 297.pp, 2015. (Available  
393 from  
394 [http://www.godac.jamstec.go.jp/catalog/data/doc\\_catalog/media/MR15-03\\_leg1\\_all.pdf](http://www.godac.jamstec.go.jp/catalog/data/doc_catalog/media/MR15-03_leg1_all.pdf))
- 395 Thorne, P. W., Parker, D. E., Tett, S. F. B., Jones, P. D., McCarthy, M., Coleman, H., and  
396 Brohan, P.: Revisiting radiosonde upper air temperatures from 1958 to 2002, J. Geophys.  
397 Res., 110, D18105, doi:10.1029/2004JD005753, 2005.
- 398 Vömel, H., Selkirk, H., Miloshevich, L., Valverde-Canossa, J., Valdés, J., Kyrö, E., Kivi, R.,  
399 Stolz, W., Peng, G., and Diaz, J. A.: Radiation dry bias of the Vaisala RS92 humidity  
400 sensor, J. Atmos. Ocean. Tech., 24, 953-963, doi:10.1175/JTECH2019.1, 2007.
- 401 Yang, G.-Y., and Slingo, J.: The diurnal cycle in the tropics, Mon. Wea. Rev., 129, 784-801,  
402 doi:10.1175/1520-0493(2001)129<0784:TDCITT>2.0.CO;2, 2001.
- 403 Yoneyama, K., Hanyu, M., Sueyoshi, S., Yoshiura, F., and Katsumata, M.: Radiosonde  
404 observation from the ship in the tropical region, Report of Japan Marine Science and  
405 Technology Center, 45, 31-39, 2002. (Available from  
406 [http://www.jamstec.go.jp/res/ress/yoneyamak/PDFs/Yoneyama-etal\\_2002\\_JAMSTECR.](http://www.jamstec.go.jp/res/ress/yoneyamak/PDFs/Yoneyama-etal_2002_JAMSTECR.pdf)  
407 pdf)
- 408 Yoneyama, K., Fujita, M., Sato, N., Fujiwara, M., Inai, Y., and Hasebe, F.: Correction for  
409 radiation dry bias found in RS92 radiosonde data during the MISMO field experiment,



410 SOLA, 4, 13-16, doi:10.2151/sola.2008-004, 2008.

411 Yu, H., Ciesielski, P. E., Wang, J., Kuo, H.-C., Vömel, H., and Dirksen, R.: Evaluation of  
412 humidity correction methods for Vaisala RS92 tropical sounding data, *J. Atmos. Ocean.*  
413 *Tech.*, 32, 397–411, doi:10.1175/JTECH-D-14-00166.1, 2015.

414

415



416 **Table 1.** Nominal accuracies of the radiosondes according to the manufacturer.

417

		RS41-SGP	RS92-SGPD
Weight		113 g	280 g
Combined uncertainty in sounding (2-sigma confidence level (95.5 %) cumulative uncertainty)	Temperature	0.3°C < 16 km 0.4°C > 16 km	0.5°C
	Relative humidity	4 %RH	5 %RH
Reproducibility in sounding (standard deviation of differences in twin soundings)	Pressure		1.0 > 100 hPa 0.6 < 100 hPa
	Temperature <sup>a</sup>	0.15°C > 100 hPa 0.30°C < 100 hPa	0.2°C > 100 hPa 0.3°C 100–20 hPa 0.5°C < 20 hPa
	Relative humidity <sup>a</sup>		2 %RH
	Pressure		0.5 > 100 hPa 0.3 < 100 hPa
	Wind speed		0.15 m/s
	Wind direction <sup>b</sup>		2°

418 <sup>a</sup> Ascent rate above 3 m s<sup>-1</sup>

419 <sup>b</sup> Wind speed above 3 m s<sup>-1</sup>

420



421 **Table 2.** Date, position (latitude and longitude), and surface meteorological state (pressure,  
 422 temperature, relative humidity, wind direction, and wind speed) when each  
 423 twin-radiosonde was launched. Line under time denotes nighttime.  
 424

No.	Date	Time (UTC)	Lat. (°N)	Lon. (°E)	Pressure (hPa)	Temp. (°C)	RH (%)	Wind dire. (°)	Wind speed (m s <sup>-1</sup> )	Maximum height (m)	Mean ascent rate (m s <sup>-1</sup> )
1	27 Aug.	23:30	40.170	149.944	1011.7	15.9	69	23	7.1	26,734	4.06
2	28 Aug.	23:30	42.423	153.413	1010.7	14.0	70	306	11.2	23,328	4.42
3	29 Aug.	23:30	44.831	157.193	1004.2	12.1	93	289	11.6	21,607	4.45
4	31 Aug.	23:32	49.931	165.753	999.6	10.9	93	275	5.6	19,380	4.74
5	2 Sep.	23:30	55.493	175.342	1000.4	10.3	97	155	7.8	13,617	4.68
6	4 Sep.	23:32	63.429	-172.917	1008.6	9.0	81	294	3.6	23,554	5.06
7	7 Sep.	5:30	71.054	-166.937	1015.9	1.3	83	342	6.7	22,872	5.22
8	12 Sep.	23:30	72.476	-156.289	1009.8	-0.1	96	91	9.3	21,243	5.36
9	16 Sep.	5:30	72.341	-156.183	1015.1	-1.7	86	46	5.4	22,298	5.33
10	24 Sep.	23:31	73.209	-157.801	993.2	0.7	95	170	9.8	25,309	5.12
11	28 Sep.	17:31	74.369	-166.569	987.8	-1.4	92	164	8.6	23,291	5.18
12	28 Sep.	23:30	74.466	-168.184	982.0	-0.9	70	167	11.2	22,811	5.26
13	29 Sep.	5:30	74.002	-168.755	979.9	-2.3	80	210	9.9	19,338	5.25
14	30 Sep.	<u>11:30</u>	70.379	-168.755	993.2	-2.1	89	282	7.0	19,897	5.16
15	30 Sep.	23:30	68.061	-168.829	1008.6	1.8	69	296	7.1	22,613	5.17
16	4 Oct.	23:30	60.742	-167.777	1011.4	8.1	100	186	14.3	19,498	4.77
17	11 Oct.	23:30	53.639	178.824	1006.8	6.3	90	10	3.8	25,051	5.17
18	17 Oct.	23:30	41.790	154.884	1019.8	12.0	64	177	2.9	25,928	5.21
19	10 Nov.	5:38	23.565	136.761	1011.6	26.7	83	357	3.3	25,395	3.78
20	11 Nov.	5:39	19.210	134.811	1011.6	28.0	81	72	8.1	26,589	4.04
21	30 Nov.	8:29	-4.076	101.885	1006.2	28.5	75	202	4.2	22,184	3.95
22	1 Dec.	5:30	-4.051	101.887	1008.1	28.4	79	298	2.7	26,510	4.27
23	3 Dec.	5:29	-4.067	101.893	1008.5	28.0	82	275	4.2	28,867	4.35
24	5 Dec.	2:30	-4.069	101.883	1009.5	26.0	92	254	1.9	28,016	4.07
25	5 Dec.	<u>17:45</u>	-4.085	101.893	1008.6	27.4	86	80	1.3	26,822	3.98
26	6 Dec.	<u>20:26</u>	-4.067	101.910	1005.8	27.9	85	139	6.2	27,518	3.97
27	8 Dec.	<u>14:29</u>	-4.079	101.890	1010.5	27.9	82	126	3.0	26,965	4.26
28	9 Dec.	2:28	-4.053	101.887	1010.0	27.4	81	298	1.9	27,123	4.32
29	10 Dec.	<u>17:27</u>	-4.042	101.890	1009.1	27.0	87	6	1.4	24,650	4.40



30	11 Dec.	<u>14:20</u>	-4.053	101.873	1008.0	25.5	98	5	10.3	15,050	6.62
31	13 Dec.	<u>20:28</u>	-4.059	101.894	1006.1	28.1	77	324	6.2	20,798	3.57
32	15 Dec.	5:28	-4.045	101.896	1007.9	27.6	82	339	8.6	23,698	4.25
33	16 Dec.	2:50	-4.057	101.886	1010.3	25.0	94	310	5.2	4,803	2.48
34	16 Dec.	<u>14:22</u>	-4.062	101.889	1010.1	26.2	90	11	7.9	21,629	4.48
35	17 Dec.	5:28	-4.053	101.896	1008.2	28.2	72	278	1.4	21,607	3.61
36	17 Dec.	<u>20:27</u>	-5.173	101.413	1007.2	28.2	79	303	6.0	24,944	3.70

425

426



427 **Table 3.** Biases, RMS difference, and standard deviations (SD) of the variables between  
 428 the RS92 and RS41 radiosondes. The bias is the mean of RS92 – RS41 differences.  
 429

Variable	Total		MR15-03 (Subarctic – Arctic)		MR15-04 (Subtropics – Tropics)	
	Bias	RMS SD	Bias	RMS SD	Bias	RMS SD
	Temperature (°C)	+0.04	0.17	+0.01	0.15	+0.06
$P_{RS92} > 100\text{hPa}$		0.17		0.15		0.18
Temperature (°C)	-0.01	0.22	-0.10	0.27	+0.05	0.18
$P_{RS92} < 100\text{hPa}$		0.22		0.25		0.17
Pressure (hPa)	+0.52	0.67	+0.41	0.58	+0.64	0.76
$P_{RS92} > 100\text{hPa}$		0.42		0.40		0.41
Pressure (hPa)	+0.55	0.67	+0.57	0.61	+0.53	0.71
$P_{RS92} < 100\text{hPa}$		0.38		0.21		0.47
Relative humidity (%)	-0.89	3.14	-0.50	2.14	-1.26	3.86
		3.01		2.08		3.64
Zonal wind speed ( $\text{m s}^{-1}$ )	-0.0017	0.18	+0.0027	0.17	-0.0059	0.18
		0.18		0.17		0.18
Meridional wind speed ( $\text{m s}^{-1}$ )	-0.0051	0.17	+0.0104	0.18	-0.0199	0.16
		0.17		0.18		0.15

430  
 431



432 **Table 4.** Bias correction table of relative humidity that was created by matching the CDFs  
 433 from the RS92 data to the RS41 data (%RH) based on the daytime data obtained during  
 434 the MR15-04 cruise.

435

	$\leq -80^{\circ}\text{C}$	$-60^{\circ}\text{C}$	$-40^{\circ}\text{C}$	$-20^{\circ}\text{C}$	$0^{\circ}\text{C}$	$\geq 20^{\circ}\text{C}$
2.5 %RH	1.84	0	-0.42	0	0	0
7.5	0.50	2.35	0.50	0.25	0.36	0
12.5	4.12	2.14	3.24	1.15	0.79	0
17.5	6.47	3.13	2.31	1.43	1.00	0
22.5	7.14	3.33	2.86	1.67	1.67	0
27.5	8.93	1.67	4.09	2.50	1.82	0
32.5	8.13	2.50	4.23	3.00	0.88	0
37.5	7.31	2.50	4.33	2.92	4.17	1.67
42.5	6.25	4.06	4.38	2.73	3.75	0.63
47.5	7.50	5.00	2.50	2.78	2.08	4.17
52.5	5.00	5.50	4.17	2.65	1.67	2.14
57.5	0	4.50	5.00	4.09	2.00	1.25
62.5	0	5.00	2.22	5.00	2.76	2.50
67.5	0	5.00	0	4.44	0.80	0.49
72.5	0	0	0	3.27	1.60	1.25
77.5	0	0	0	3.38	1.35	1.44
82.5	0	0	0	2.50	1.45	1.36
87.5	0	0	0	3.00	1.73	0.91
92.5	0	0	0	2.50	0.90	0.56
97.5	0	0	0	0	0	0

436

437



438

## Figure Captions

439 **Figure 1.** Positions of the twin-radiosonde launches during the (a) MR15-03 cruise, and (b)  
440 MR15-04 cruise. (c) Time-latitude diagram of the launches. Black and red dots represent  
441 daytime and nighttime soundings, respectively.

442

443 **Figure 2.** Photographs of (upper) the RS92 and RS41 radiosondes directly attached to  
444 each other and (lower) a launch on R/V *Mirai*.

445

446 **Figure 3.** Vertical profiles of the median (black), 25–75th percentile (green), 10–90th  
447 percentile (gray), and mean  $\pm$  standard deviation (cyan) of all differences between the  
448 RS92 and RS41 observations (RS92 – RS41) for (a) pressure, (b) temperature, (c)  
449 relative humidity, (d) zonal wind, and (e) meridional wind.

450

451 **Figure 4.** Mean difference in relative humidity between the RS92 and RS41 radiosondes  
452 (RS92 – RS41) as a function of the RS41 temperature for relative humidity ranges of  
453 0–20 % (blue), 20–40 % (red), 40–60 % (green), 60–100 % (black), and 0–100 % (gray).

454

455 **Figure 5.** Vertical profiles of the RS41 temperature (red), RS92 temperature (blue), RS41  
456 relative humidity (magenta), and RS92 relative humidity (cyan). (a) Flight No. 29  
457 launched at 1727 UTC on 10 December 2015 in the tropics, and (b) Flight No. 9 launched



458 at 0530 UTC on 16 September 2015 in the Arctic.

459

460 **Figure 6.** Same as Fig. 5, but for (a) Flight No. 30 launched at 1420 UTC on 11 December  
461 2015, (b) Flight No. 22 launched at 0530 UTC on 1 December 2015, and (c) Flight No. 23  
462 launched at 0529 UTC on 3 December 2015. All launches in the tropics.

463

464 **Figure 7.** Differences between the RS92 and RS41 radiosonde (RS92 – RS41) results for  
465 daytime (blue) and nighttime (red) flights during the MR15-04 cruise for (a) pressure, (b)  
466 temperature, and (c) relative humidity.

467

468 **Figure 8.** Relative difference between the RS92 and RS41 relative humidity obtained  
469 during the daytime on the MR15-04 cruise (blue dots, %). Relative difference is defined  
470 as the relative humidity difference expressed as a percentage of the RS41 relative  
471 humidity. Green line denotes the median of the relative difference. Lower panel shows an  
472 enlargement of part of the upper panel.

473

474 **Figure 9.** (a) CDFs of relative humidity for the RS92 (bold dashed line) and RS41 (bold  
475 solid line) data in the temperature range of  $-90$  to  $-70^{\circ}\text{C}$ . The daytime data obtained  
476 during the MR15-04 cruise were used. Thin solid lines illustrate the CDF-matching  
477 technique (see text). (b) Bias correction of relative humidity for the same temperature



478 range.

479

480 **Figure 10.** Medians of the relative humidity difference between the RS92 and RS41

481 radiosondes obtained during the daytime on the MR15-04 cruise. Blue and black lines

482 show the profiles before and after the bias correction of the RS92 data.

483

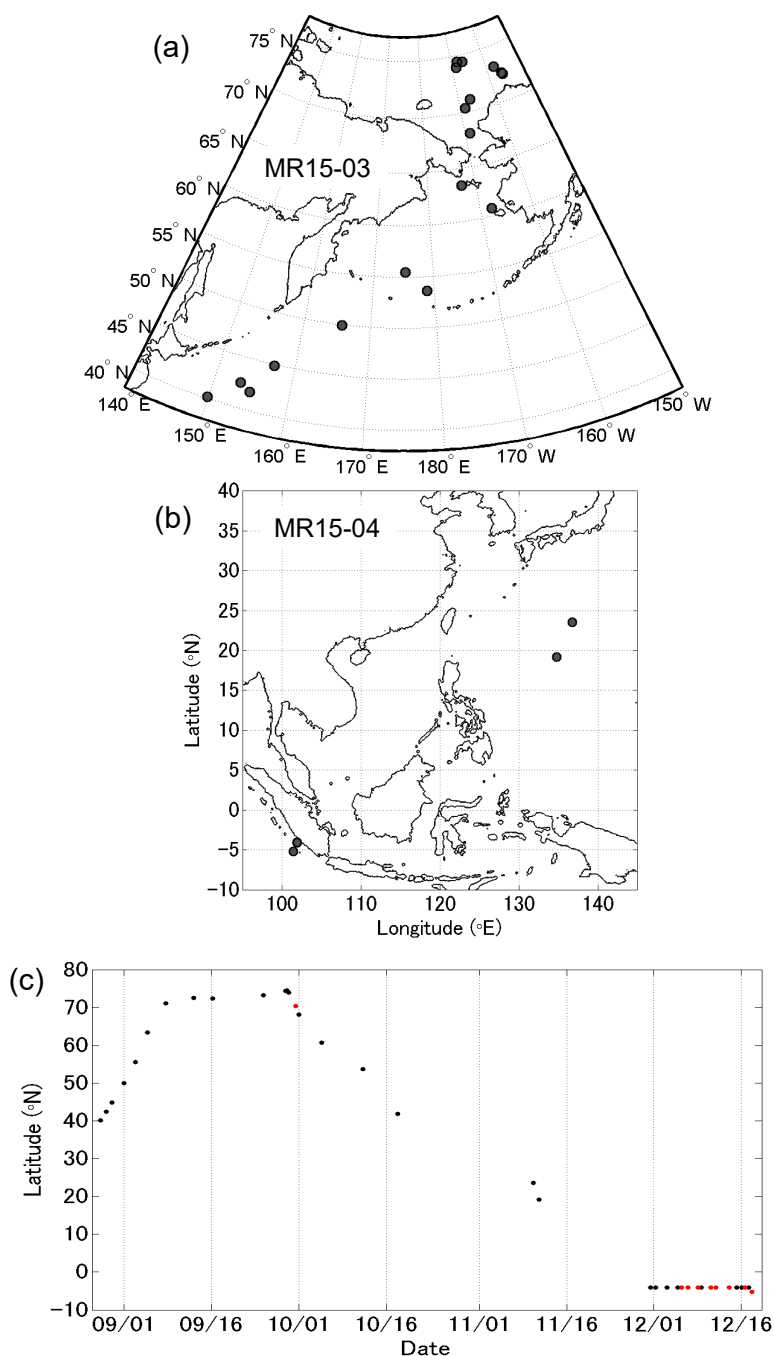


Fig. 1. Positions of the twin-radiosonde launches during the (a) MR15-03 cruise, and (b) MR15-04 cruise. (c) Time-latitude diagram of the launches. Black and red dots represent daytime and nighttime soundings, respectively.



Fig.2. Photographs of (upper) the RS92 and RS41 radiosondes directly attached to each other and (lower) a launch on R/V *Mirai*.

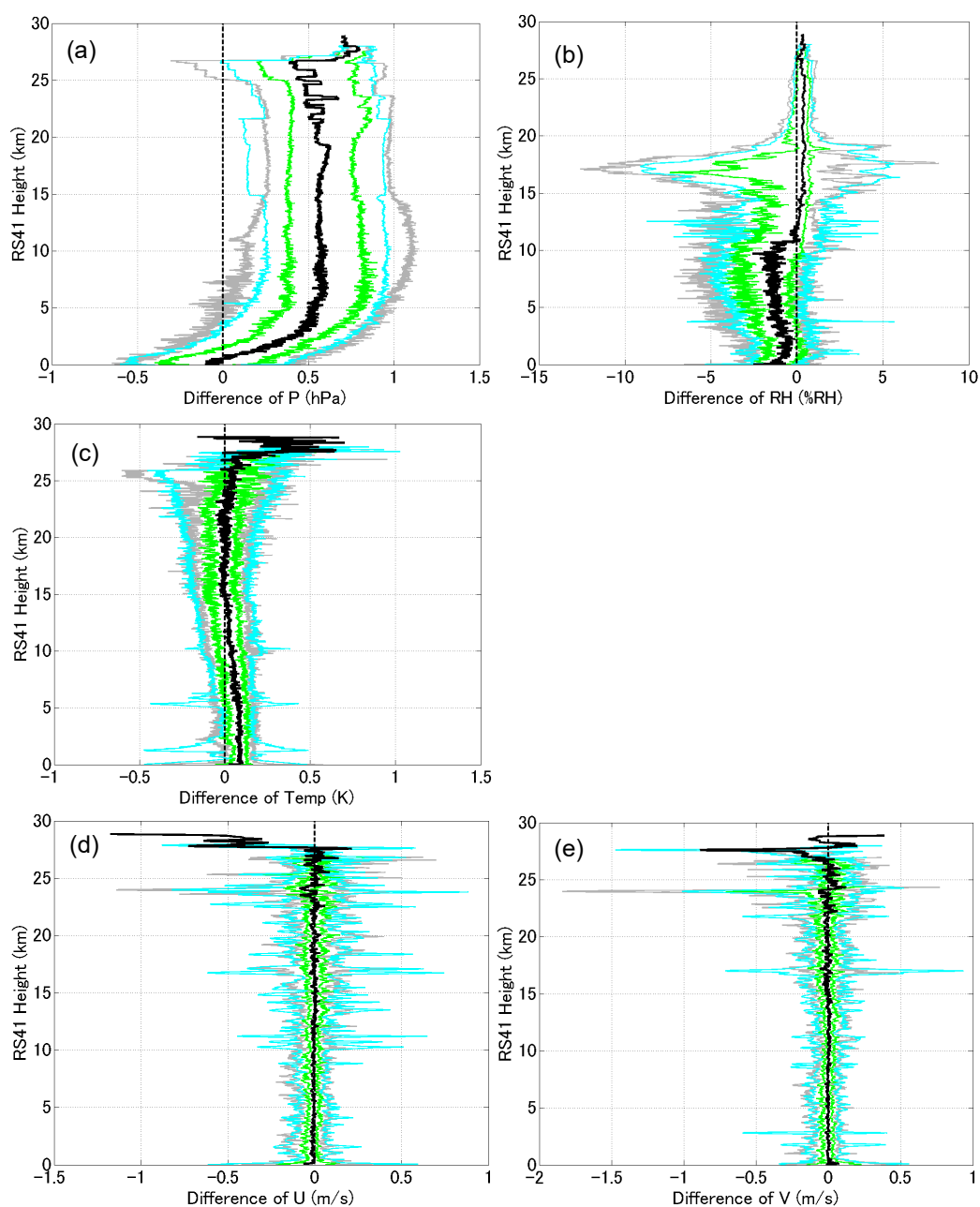


Fig.3. Vertical profiles of the median (black), 25–75th percentile (green), 10–90th percentile (gray), and mean  $\pm$  standard deviation (cyan) of all differences between the RS92 and RS41 observations (RS92 – RS41) for (a) pressure, (b) temperature, (c) relative humidity, (d) zonal wind, and (e) meridional wind.

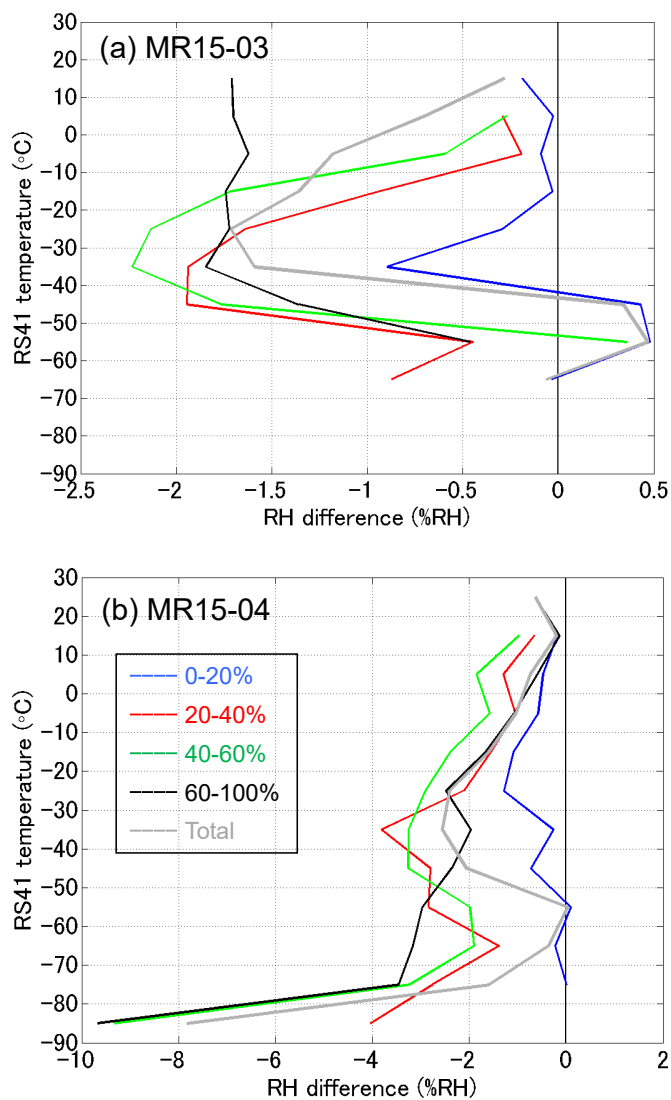


Fig.4. Mean difference in relative humidity between the RS2 and RS41 radiosondes (RS2 – RS41) as a function of the RS41 temperature for relative humidity ranges of 0–20 % (blue), 20–40 % (red), 40–60 % (green), 60–100 % (black), and 0–100 % (gray).

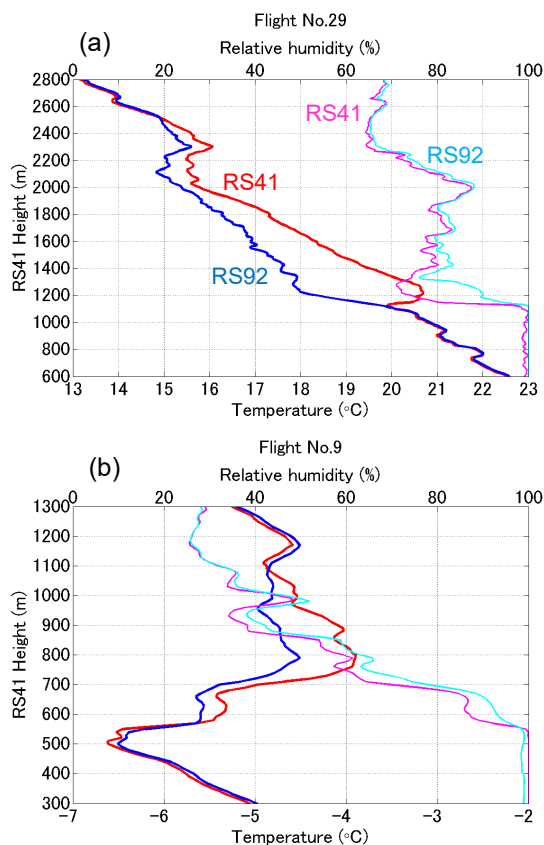


Fig.5. Vertical profiles of the RS41 temperature (red), RS92 temperature (blue), RS41 relative humidity (magenta), and RS92 relative humidity (cyan). (a) Flight No. 29 launched at 1727 UTC on 10 December 2015 in the tropics, and (b) Flight No. 9 launched at 0530 UTC on 16 September 2015 in the Arctic.

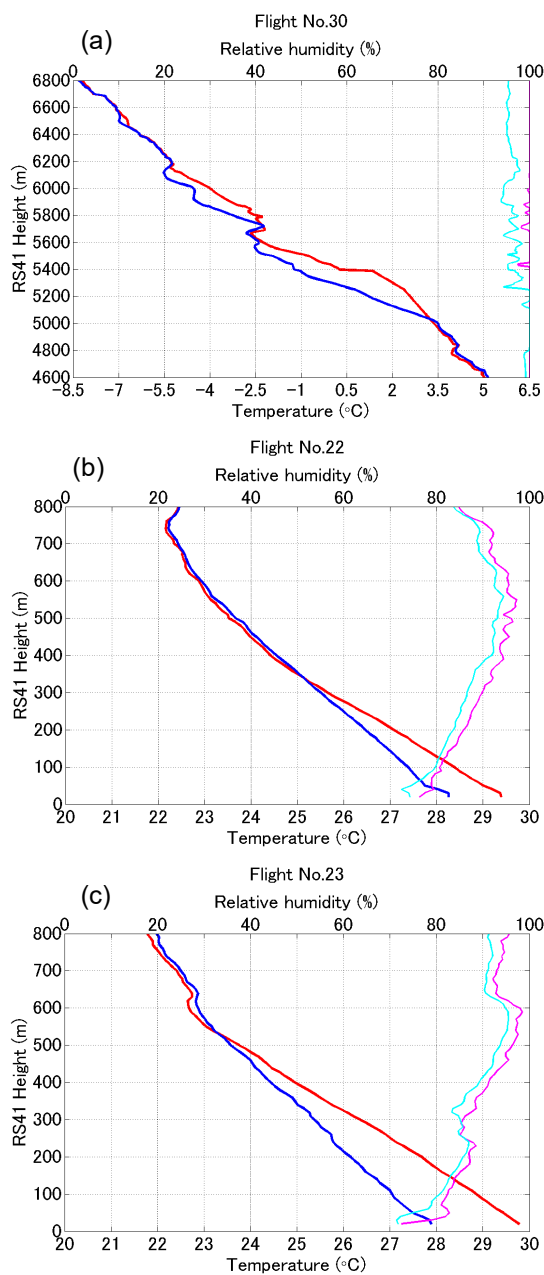


Fig.6. Same as Fig. 5, but for (a) Flight No. 30 launched at 1420 UTC on 11 December 2015, (b) Flight No. 22 launched at 0530 UTC on 1 December 2015, and (c) Flight No. 23 launched at 0529 UTC on 3 December 2015. All launches in the tropics.

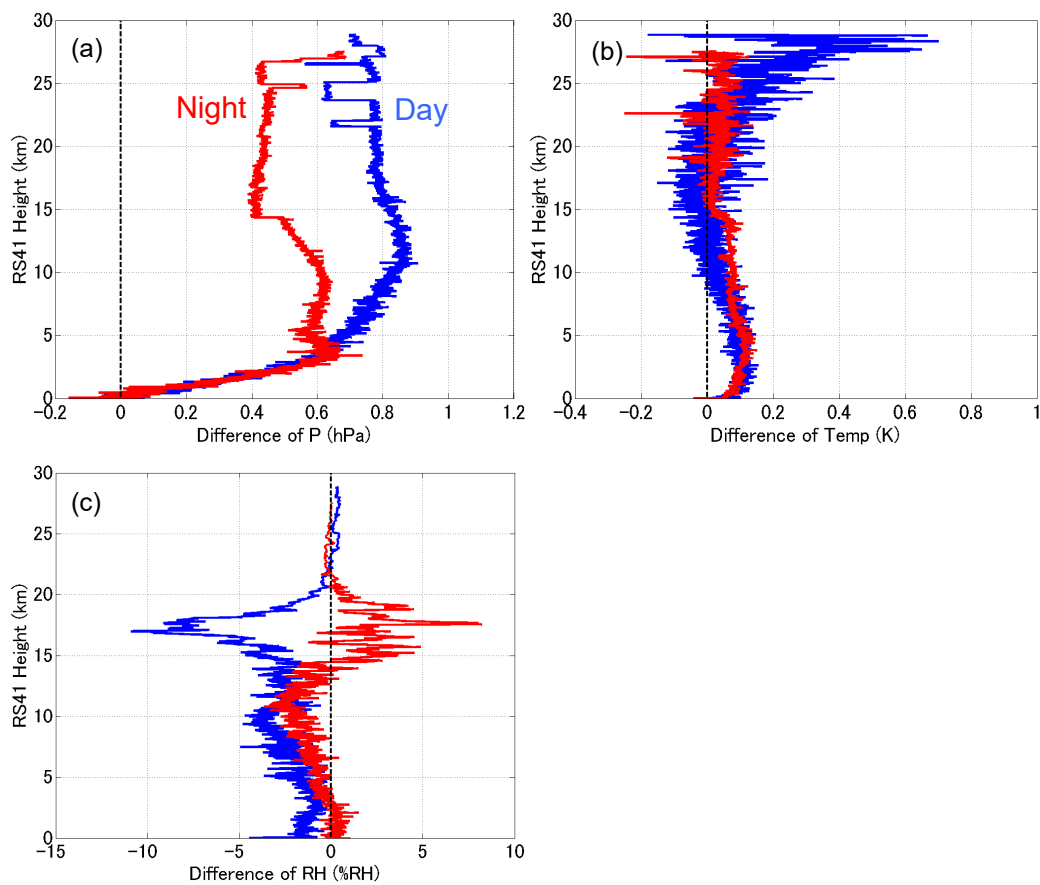


Fig.7. Differences between the RS92 and RS41 radiosonde (RS92 – RS41) results for daytime (blue) and nighttime (red) flights during the MR15-04 cruise for (a) pressure, (b) temperature, and (c) relative humidity.

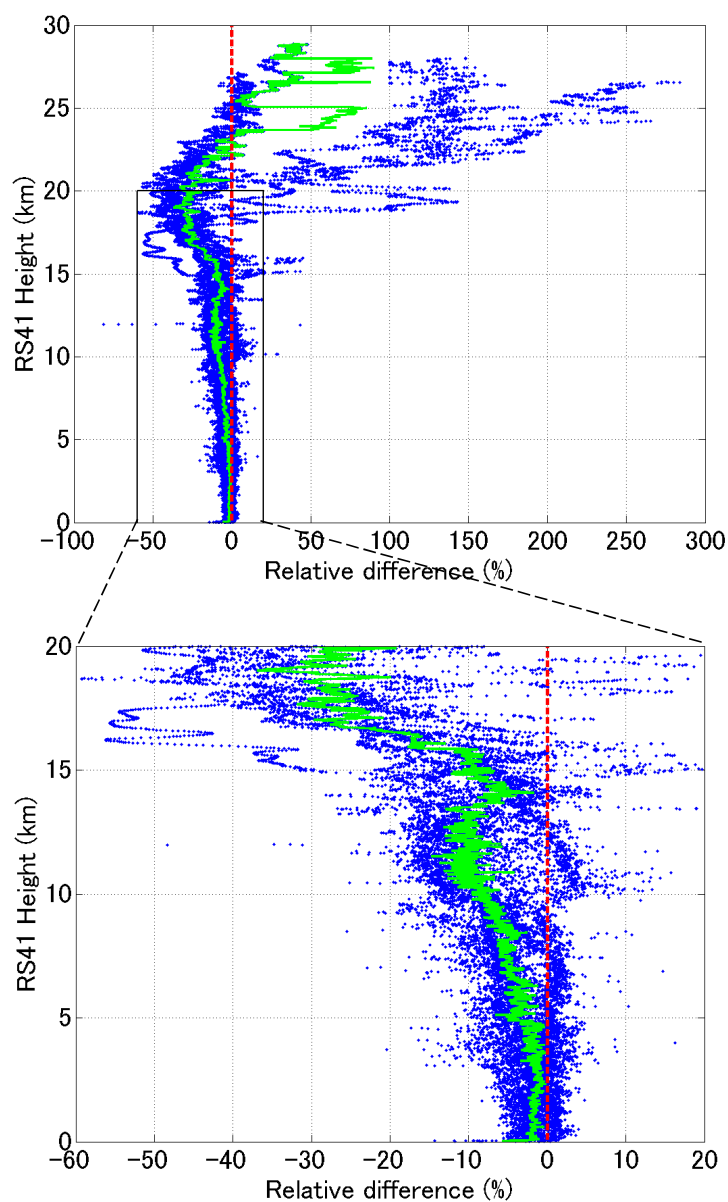


Fig. 8. Relative difference between the RS92 and RS41 relative humidity obtained during the daytime on the MR15-04 cruise (blue dots, %). Relative difference is defined as the relative humidity difference expressed as a percentage of the RS41 relative humidity. Green line denotes the median of the relative difference. Lower panel shows an enlargement of part of the upper panel.

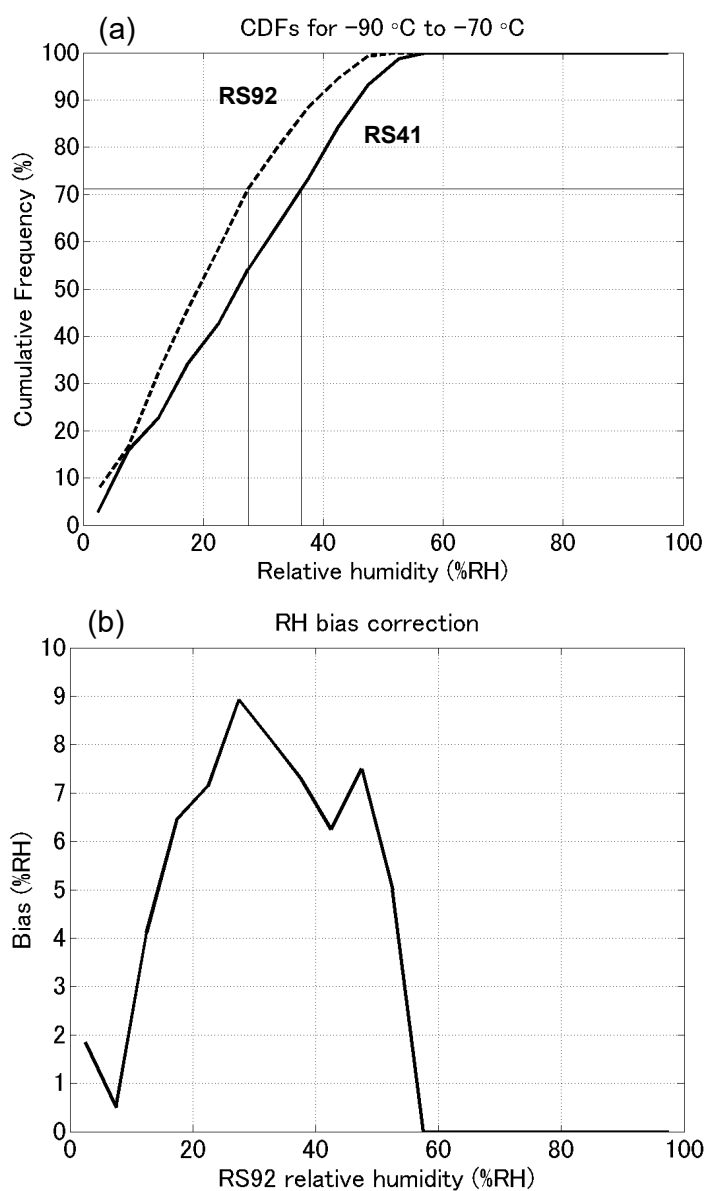


Fig. 9. (a) CDFs of relative humidity for the RS92 (bold dashed line) and RS41 (bold solid line) data in the temperature range of  $-90$  to  $-70$  °C. The daytime data obtained during the MR15-04 cruise were used. Thin solid lines illustrate the CDF-matching technique (see text). (b) Bias correction of relative humidity for the same temperature range.

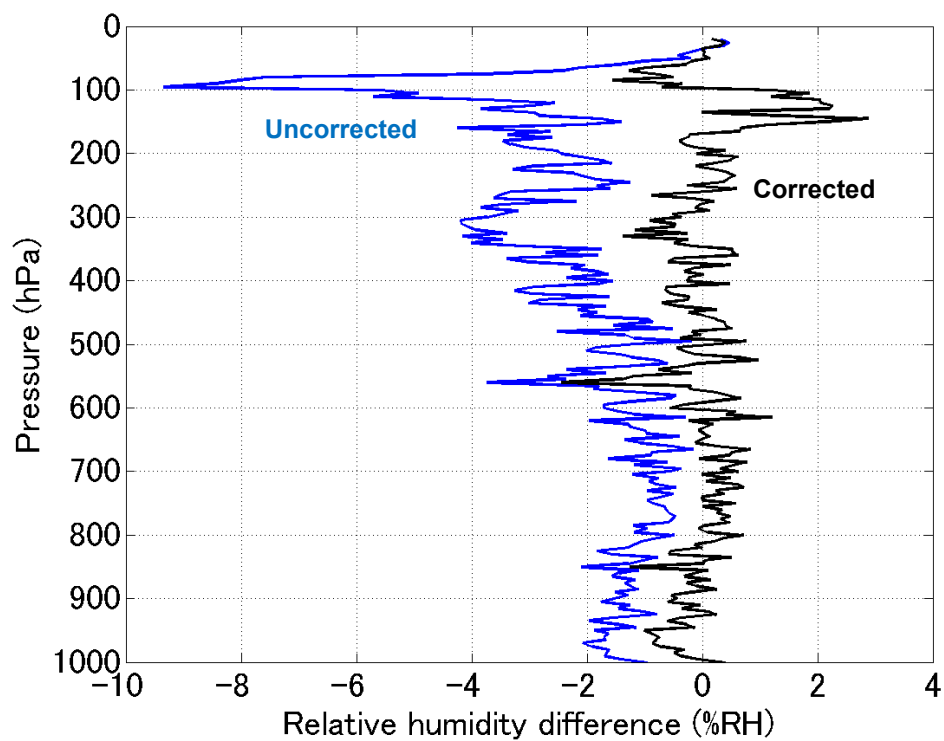


Fig. 10. Medians of the relative humidity difference between the RS92 and RS41 radiosondes obtained during the daytime on the MR15-04 cruise. Blue and black lines show the profiles before and after the bias correction of the RS92 data.